Cancer Cell
Article

Persistence of Leukemia-Initiating Cells in a Conditional Knockin Model of an Imatinib-Responsive Myeloproliferative Disorder

Katherine I. Oravecz-Wilson,[1,4] Steven T. Philips,[1,4] Ömer H. Yilmaz,[1,4] Heather M. Ames,[1] Lina Li,[1] Brendan D. Crawford,[1] Alice M. Gauvin,[1] Peter C. Lucas,[2] Kajal Sitwala,[2] James R. Downing,[3] Sean J. Morrison,[1] and Theodora S. Ross[1,*]
[1]Department of Internal Medicine
[2]Department of Pathology
University of Michigan Medical School, Ann Arbor, MI 48109, USA
[3]Department of Pathology, St Jude Children's Research Hospital, Memphis, TN 38105, USA
[4]These authors contributed equally to this work
*Correspondence: tsross@umich.edu
DOI 10.1016/j.ccr.2009.06.007

SUMMARY

Despite remarkable responses to the tyrosine kinase inhibitor imatinib, CML patients are rarely cured by this therapy perhaps due to imatinib refractoriness of leukemia-initiating cells (LICs). Evidence for this is limited because of poor engraftment of human CML-LICs in NOD-SCID mice and nonphysiologic expression of oncogenes in retroviral transduction mouse models. To address these challenges, we generated mice bearing conditional knockin alleles of two human oncogenes: HIP1/PDGFβR (H/P) and AML1-ETO (A/E). Unlike retroviral transduction, physiologic expression of H/P or A/E individually failed to induce disease, but coexpression of both H/P and A/E led to rapid onset of a fully penetrant, myeloproliferative disorder, indicating cooperativity between these two alleles. Although imatinib dramatically decreased disease burden, LICs persisted, demonstrating imatinib refractoriness of LICs.

INTRODUCTION

A number of chromosomal translocations that contribute to leukemogenesis in humans have been identified (Gilliland, 2002). For example, translocations that lead to the expression of a constitutively active platelet-derived growth factor beta receptor (PDGFβR) fusion protein, such as HIP1/PDGFβR (H/P) (Ross et al., 1998), contribute to the development of chronic myelomonocytic leukemia (CMML) (Grand et al., 2004). Although these PDGFβR-driven leukemias are clinically sensitive to imatinib therapy (Tefferi and Gilliland, 2007), the leukemias can still progress to acute myeloid leukemia (AML) or bone marrow failure over time. Progression to AML in chronic leukemias with tyrosine kinase mutations is associated not only with resistance to imatinib but also with additional genetic lesions such as the t(8;21)-associated AML1/ETO (A/E) fusion protein (Golub et al., 1994; Miyoshi et al., 1991).

Molecularly targeted cancer therapies, such as imatinib, have revolutionized patient care over the past 20 years. These drugs target molecular defects specific to cancer cells rather than simply targeting mitotically active cells. For example, the use of imatinib in CML patients has led to an enormous reduction in the 5-year mortality associated with Bcr/Abl-positive CML (Druker et al., 2006); however, only 5% of patients maintained on imatinib therapy are considered cured as defined by a molecular remission (Kavalerchik et al., 2008). In fact, upon discontinuation of therapy, the disease aggressively relapses in the majority of patients (Savona and Talpaz, 2008). These clinical observations suggest that although imatinib eliminates the bulk of CML cells, this drug probably does not eliminate

SIGNIFICANCE

Tyrosine kinase oncogenes contribute to the development and maintenance of many neoplasms. To understand how these oncogenes contribute to drug sensitivity and development of neoplasms, realistic mouse models are essential. A conditional knockin allele of the HIP1/PDGFβR tyrosine kinase oncogene that allows for physiologic levels of HIP1/PDGFβR (single copy, endogenous promoter) at the right time (adult) and place (cell type) is described here. This model allows for the testing of therapies that target PDGFβR oncogene-activated pathways in immunocompetent animals with leukemia. Using these animals, we have found that HIP1/PDGFβR;AML1/ETO-expressing leukemia-initiating cells are relatively refractory to imatinib. These data provide direct evidence that rare leukemia-initiating cells in CML are more resistant to imatinib treatment than other CML cells.

the leukemia-initiating cells (LICs) that maintain the disease state.

The CML-LIC, like normal hematopoietic stem cells (HSCs), is thought to have not only the properties of self-renewal and multipotentiality, but also a relative quiescence compared to the more differentiated leukemia cells (Kavalerchik et al., 2008). This quiescence has led to the hypothesis that the LIC is likely to be refractory to nontargeted therapies, such as chemotherapy or radiotherapy, which depend upon cell division for their cytotoxicity. In contrast, targeted therapies, such as imatinib, were thought to be more likely than standard therapy approaches to eliminate LICs. Unfortunately, in the case of CML, the latter does not appear to be the case. Indeed, cell culture data have suggested that Bcr/Abl-expressing cells are refractory to imatinib therapy when quiescent and that awakening these cells increases their sensitivity to this drug (Jorgensen et al., 2006). The mechanism of this observed resistance and the in vivo confirmation of the relative refractoriness of CML-LICs to imatinib therapy compared with the bulk of neoplastic cells, however, have not yet been reported. These types of in vivo studies have been difficult to accomplish due to poor engraftment of CML LICs into NOD-SCID mice and limitations inherent in the variability associated with studying human subjects.

Modeling hematopoietic neoplasias in mice to study effects of therapies on cancer cells in vivo has also been challenging because the consequences of oncogene expression are different depending upon the techniques used to obtain expression. For instance, retroviral overexpression of A/E in hematopoietic cells leads to the formation of acute leukemias in some cases but not in others, and this variability might be due, in part, to expression of different isoforms (Yan et al., 2006). This heterogeneity in outcome might also stem from variables inherent to retrovirus-mediated transduction, including copy number, expression level, integration site, the presence and identity of cooperating insertional mutations, and the identity of the infected cells. Furthermore, growth of retrovirally infected cells might select for rare clones that have the highest levels of proliferation. In contrast to the retroviral model of A/E, Downing and colleagues developed a conditional knockin allele of A/E that was expressed from the mouse *Aml1* locus. Conditional expression of A/E under the control of native regulatory elements in the locus was never leukemogenic on its own. Treatment of disease-free conditional A/E knockin mice with the DNA alkylating mutagen *N*-ethyl-*N*-nitrosourea (ENU) resulted in the development of acute leukemia (Higuchi et al., 2002). These results suggest that the use of knockin alleles of oncogenes improves leukemia mouse modeling by achieving more realistic expression patterns; however, the A/E knockin model was still not entirely useful to leukemia investigators because these mice require unidentified cooperating mutations to develop a neoplastic phenotype.

In contrast to the existence of conditional knockin mouse models of the transcription factor oncogene A/E (Higuchi et al., 2002) and other transcription factor oncogenes such as the MLL translocation fusions (Cano et al., 2008; Chen et al., 2008), mouse models currently used to study tyrosine kinase oncogenes have been limited to retroviral transduction and transplantation assays (Grisolano et al., 2003; Neering et al., 2007), a nontargeted transgenic of BCR/ABL (Huettner et al., 2000; Jaiswal et al., 2003), and a nonconditional knockin mouse model of Flt3-Itd mutations (Lee et al., 2007; Li et al., 2008). Similar to the results described above for A/E, Flt3-Itd knockin animals demonstrated that knockin alleles of oncogenic tyrosine kinases likely yield different results than retrovirally expressed alleles (Lee et al., 2007; Li et al., 2008). Thus, most conclusions as they relate to oncogene expression-induced leukemias to date have been based on nonphysiologic expression of oncogenes. Our understanding of leukemia biology will clearly benefit from studying the consequences of oncogene expression under the control of native regulatory elements.

Because a knockin allele of an oncogenic PDGFβR kinase that is conditionally expressed under the control of native regulatory elements in adult hematopoietic progenitors is not yet available, the goals of this study were to generate a conditional knockin allele of the H/P mutation and examine its ability to drive hematopoietic neoplasias. This allele might provide us with a more realistic model of X-PDGFβR-driven hematopoietic neoplasias for investigation of therapies. Another goal of this study was to test if knocked in tyrosine kinase oncogene alleles can cooperate with knocked in transcription factor oncogene alleles such as A/E (Higuchi et al., 2002). Finally, we used these H/P knockin mice to compare the response of LICs and other neoplastic cells to imatinib therapy.

RESULTS

Generation of H/P Conditional "Knockin" Mice

To model the human t(5;7) translocation, we engineered the human H/P cDNA into the mouse *Hip1* locus downstream of a *loxP*-bracketed transcriptional stop cassette (*Hip1*$^{LSL\text{-}H/P}$, Figure 1A). This conditional knockin allele allows use of specific Cre transgenic mice to guide tissue-specific expression together with the endogenous mouse *Hip1* promoter to regulate the expression of the oncogenic fusion protein both spatially and temporally. We targeted ES cells to generate mice carrying the *Hip1*$^{LSL\text{-}H/P}$ allele (Figure 1B). *Hip1*$^{+/LSL\text{-}H/P}$ mice were born at predicted Mendelian frequency and exhibited normal growth curves; however, these mice were distinguishable from wild-type littermates by the presence of gross micro-ophthalmia and cataracts as seen previously in the heterozygous *Hip1*$^{+/null}$ mice (Oravecz-Wilson et al., 2004). The *Hip1*$^{+/LSL\text{-}H/P}$ mice were crossed with transgenic Mx1-Cre mice. The Mx1 promoter is activated by interferon, which is induced by treatment with the synthetic double-stranded RNA, polyinosinic-polycytidylic acid (pIpC) (Higuchi et al., 2002; Kuhn et al., 1995; Yilmaz et al., 2006). The pIpC treatment leads to Cre expression in an array of hematopoietic and nonhematopoietic cells, but because the expression of the knockin allele depends on many of the natural regulatory elements of the HIP1 locus, we predicted that its expression would closely mimic that found in the original CMML patient. Southern blot analyses demonstrated that pIpC-induced recombination occurred in liver, kidney, and spleen but not in brain or testes (Figure 1C).

Absence of Neoplasia in pIpC-Induced Mx1-Cre;*Hip1*$^{+/LSL\text{-}H/P}$ Mice

Mx1-Cre;Hip1$^{+/LSL\text{-}H/P}$ and *Mx1-Cre;Hip1*$^{+/+}$ littermate controls were treated with pIpC at 6 weeks of age (n = 20 for each

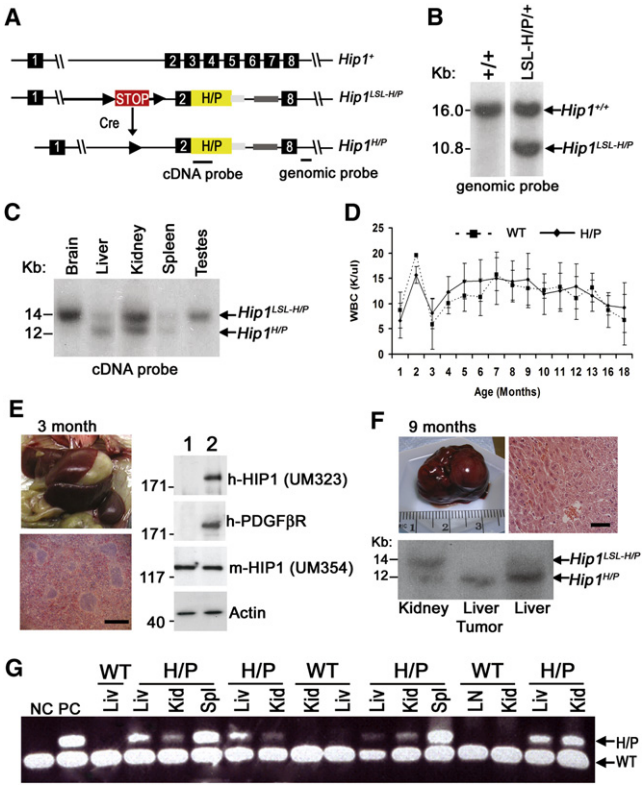

Figure 1. Phenotype of pIpC-Induced Mx1.Cre;*Hip1*$^{+/LSL-H/P}$ Mice

(A) Schematic of the first 8 of 32 exons of the murine *Hip1* genomic locus (*Hip1*$^{+}$), the targeted *Hip1*$^{LSL-H/P}$ knockin allele generated by homologous recombination, and the allele with a deleted stop cassette (*Hip1*$^{H/P}$) following Cre-mediated recombination. The following features are indicated: stop cassette bracketed by *loxP* recombination sequences (LSL), partial human H/P cDNA, and cDNA or genomic hybridization probes. Just 3′ of the H/P cDNA is a poly A tail (light gray box) and 3′ of this was a neomycin selection cassette (dark gray box).

(B) Southern blot analysis (genomic probe) of EcoRI-digested DNA from wild-type and Mx1Cre;*Hip1*$^{+/LSL-H/P}$ mice.

(C) Southern blot analysis (cDNA probe) of EcoRV-digested DNA from multiple tissues shows partial recombination in the kidney, liver, and spleen and no recombination in brain or testis tissue.

(D) Complete blood counts (CBC) from wild-type and single knockin H/P mice were normal. A cohort of pIpC-treated Mx1Cre;Hip1$^{+/LSL-H/P}$ mice (n = 18) and Mx1Cre;Hip1$^{+/+}$ mice (n = 18) were observed until 18 months of age. Bleeds were taken before induction and then monthly after induction. Averages and standard deviations (SD) of all 18 mice are reported. No significant differences were observed between the two groups in WBC counts or any shifts in differentials over the entire time coarse up to the final bleed. At 18 months of age the mice were euthanized and necropsied to observe any disease either by gross observation or histologically.

(E) Enlarged spleen (0.27 g) from the youngest morbid Mx1Cre;Hip1$^{H/P}$ (tag #1156, 3 months old) shows myeloproliferation. Western blot analysis for H/P expression in this mouse was performed on bone marrow culture from the same mouse (lane 2) and from its control littermate (lane 1). The bone marrow cells were cultured for 7 days in monocytic culture conditions prior to analysis (41). Anti-human HIP1 (UM323), anti-PDGFβR (BD Bioscience), anti-mouse HIP1 (UM354), and anti-actin (Sigma) polyclonal antibodies were used to detect the human fusion protein, endogenous mouse HIP1, and actin as indicated. Scale bar represents 600 μm.

(F) A liver tumor from a 9-month-old Mx1Cre;Hip1H/P mouse (tag #1151) shows a well-differentiated hepatocellular carcinoma histopathology. Southern blot analysis (cDNA probe) of EcoRV-digested DNA from kidney, "normal" gross liver, and liver tumor DNA from the second pI-pC induced Mx1Cre;Hip1+/LSL-H/P (H/P) mouse that was moribund and sacrificed at 9 months of age. Note that the DNA from the kidney was partially recombined (50%), allowing for demonstration of both alleles, while the liver tumor is fully (100%) recombined. Scale bar represents 30 μm.

(G) Analysis for recombination in tissues from 18 month old mice demonstrates that the *Hip1*$^{H/P}$ allele was not lost over time. NC, negative control wild-type DNA; PC, positive control for presence of the recombined allele. The 336 bp band is the recombined allele and the 200 bp band is the wild-type allele.

genotype) and monitored by peripheral blood analysis for 18 months (Figure 1D). Almost all of the animals survived to 1.5 years of age without gross evidence of disease, although two moribund pIpC-induced *Mx1-Cre;Hip1*$^{+/LSL-H/P}$ mice (3 and 9 months of age) were discovered. The 3-month-old had splenomegaly with a moderately effaced splenic structure (Figure 1E). The H/P fusion protein was detectable by western blot of lysates from cultured bone marrow cells from this mouse (Figure 1E, lane 2). The 9-month-old had a well-differentiated hepatocellular carcinoma (Figure 1F). Interestingly, the neoplastic liver tissue exhibited complete recombination of the *Hip1*$^{LSL-H/P}$ allele, but the kidney from this mouse maintained a 50% rate of recombination in the *Hip1*$^{LSL-H/P}$ allele (Figure 1F). The remaining mice appeared healthy up to 1.5 years of age without abnormalities in peripheral blood cell counts (Table S1).

At the experimental endpoint of 1.5 years, the mice were killed and necropsied for gross abnormalities. Eight pIpC-induced Mx1-Cre;*Hip1*$^{+/LSL-H/P}$ mice (47%) and three Mx1-Cre;*Hip1*$^{+/+}$ mice (20%) were found to have enlarged spleens (>150 mg) upon necropsy. The histology of the enlarged spleens showed signs of myeloproliferation with enlarged red pulp. Myeloproliferative disorder (MPD) was histologically diagnosed from five of the H/P (29%) and one of the wild-type (7%) enlarged spleens. An additional Mx1-Cre;*Hip1*$^{+/LSL-H/P}$ mouse had a liver tumor (Table 1). Flow cytometry and methylcellulose analyses of bone marrow from the 1.5-year-old pIpC-treated *Mx1-Cre;Hip1*$^{+/LSL-H/P}$ mice did not display significant abnormalities (data not shown; see Table S2 available online). Excision of the floxed stop cassette was detected by polymerase chain reaction (PCR) in hematopoietic tissue from the 1.5-year-old mice, indicating that the lack of significant disease was not due to selective loss of cells with the recombined *Hip1*$^{H/P}$ allele (Figure 1G). Because the pIpC-treated *Mx1-Cre;Hip1*$^{+/LSL-H/P}$ mice did not frequently develop hematopoietic malignancies even after 1.5 years, we conclude that physiologic H/P expression is not sufficient to cause hematopoietic transformation. These results are in contrast with evidence from models that rely on retroviral bone marrow transduction and transplantation (BTT) of tyrosine kinase oncogenes such as Bcr/Abl (Neering et al., 2007), TEL/PDGFβR (Grisolano et al., 2003), and H/P. For example, H/P in the BTT system induces an MPD with full penetrance and latency of 40–100 days after transplant (Figure S1). Although latencies of disease onset might be quite variable between different oncogenes (e.g., Bcr/Abl induced disease with the least latency between 21 and 28 day after transplant), all three of these oncogenes are sufficient to induce an MPD similar to CML.

The infrequent occurrence of neoplasms after a long latency in the mice bearing the H/P knockin allele suggests that additional genetic events are required to transform hematopoietic cells. To

Table 1. Neoplasms Found in H/P Mice

Aged Mice								
Genotype	n[a]	Age[b]	Liver Tumor	Lethal dis.	Large Spleen (>150 mg)	Large Thymus (>100 mg)	Mesenteric Lymphoma	Total with dis.
+/+	7	<1 yr	0	0	0	0	0	0 (0%)
H/P	6	<1 yr	1	2	1	0	0	2 (33%)
+/+	15	1.5 yr	0	0	3	0	0	3 (20%)
H/P	17	1.5 yr	1	0	8	0	0	9 (53%)
ENU-Treated Mice								
+/+	12	~1 yr	0	0	0	0	0	0 (0%)
H/P	24	~1 yr	0	7	14	4	1	17 (71%)

[a] All mice were Mx-1Cre+ and pIpC treated between 6 and 11 weeks of age.
[b] At 18 months of age, although all non-ENU treated surviving mice were apparently healthy, we did discover at necropsy that 8 of 17 remaining H/P mice had enlarged spleens compared with 3 of 15 of the wild-type mice (>150 mg).

begin to test this hypothesis, 7- to 11-week-old H/P mice were mutagenized with ENU to induce secondary mutations following pIpC induction of H/P recombination. A week after pIpC induction, the mice were treated with G-CSF for 4 days to induce myeloid proliferation, and the following day the mice were administered a single mutagenic dose of ENU (50 mg/kg). Because this dose of ENU efficiently induces only single base mutations (Breuer et al., 1991), we did not observe any neoplasias in mutagenized wild-type control animals as expected (0/12; Table 1). By contrast, 71% of the H/P-expressing mice died or developed disease by 10 months after treatment (17/24; Table 1). Disease was scored as "present" when gross thymic tumors, splenomegaly, and/or spontaneous death were observed. Interestingly, histological and fluorescence-activated cell sorting (FACS) analysis of the spleens demonstrated both myeloid and lymphoid neoplasias, suggesting that the H/P mutation does not specifically transform cells of the myeloid lineage. Finally, it remains unknown if disease penetrance in mice bearing the H/P knockin allele is modified by different genetic backgrounds because all of the studies presented here were on a pure C57/BL6 background.

CML-Like MPD in pIpC-Induced H/P;A/E Mice

The A/E mutation has been identified in many human tyrosine kinase-driven leukemias (Golub et al., 1994; Miyoshi et al., 1991; Schessl et al., 2005). We therefore tested whether conditional coexpression of the H/P and A/E fusion oncogenes from their endogenous loci in adult mice led to hematopoietic transformation. A previous report showed that Mx1-Cre-activated A/E expression from the mouse *Aml1* locus is insufficient for leukemogenesis (Higuchi et al., 2002). Dual conditional knockin mice were generated by intercrossing Mx1-Cre;*Hip1*$^{+/LSL\text{-}H/P}$ mice with *Aml1*$^{+/LSL\text{-}A/E}$ knockin mice (Figure 2A). The double knockin Mx1-Cre transgenic uninduced H/P;A/E mice, which were genotyped at weaning (Figure S2A), were born and survived at a significantly lower than predicted Mendelian frequency (7.5% observed versus 12.5% expected; $p < 0.001$ Figure S2B), indicating some embryonic or perinatal lethality. All surviving mice, however, were developmentally normal.

To study the consequences of simultaneous H/P and A/E expression in adult bone marrow, we treated H/P;A/E mice with six doses of pIpC every other day beginning at 6 weeks of age. In contrast to wild-type and single knockin mice, 100% of the induced double knockin (H/P;A/E) mice developed a fully penetrant, aggressive MPD, some within days of initiation of pIpC treatment (Figure 2B; Figure S2C). The CML-like disease was easily identifiable by severe myeloid leukocytosis (Figure 2D and 2E) and palpable hepatosplenomegaly as early as 72 hr after the start of pIpC induction (range 3–42 days; Figure 2F). White blood cell (WBC) counts at the time of euthanasia were increased an average of 25-fold above wild-type levels with a range of 50–700 K/μl (Figure 2E). Although the white cell differential demonstrated a reversal of the normal 1:3 neutrophil-to-lymphocyte ratio (Figure 2E, right), an increase in absolute numbers of all lineages was also observed. Compared with wild-type or single knockin animals, spleen and liver weights of diseased H/P;A/E animals were increased 10-fold and 2-fold, respectively (Figure 2F, left). Myeloid blasts were never observed at a frequency greater than 20% in bone marrow cytospins, precluding a diagnosis of acute leukemia (Figure S2D) (Kogan et al., 2002).

In addition, histological analysis demonstrated a gross effacement of normal splenic architecture with expansion of the red pulp (composed of sheets of mature and maturing granulocytic cells) and disappearance of organized follicles (Figure 2F, right hand panel). Mutant livers displayed similar mature myeloid cells surrounding portal cavities and infiltrating the parenchyma (Figure 2F, right hand panel). Lung sections showed infiltration of alveolar wall spaces with these same mature myeloid cells (Figure S2E). Immunohistochemical analysis demonstrated that the majority of the myeloid cells in the spleen and liver were granulocytic rather than monocytic because the cells were myeloperoxidase positive but nonspecific esterase negative (Figure S3 and data not shown). TUNEL analysis did not demonstrate changes in the frequency of apoptotic cells. In contrast, the neoplastic cells were often positive for the proliferation marker Ki67, whereas normal spleen and liver contained only rare Ki67-positive cells (Figure S3).

Although kidney, liver, and spleen displayed 50% recombination of H/P alleles in healthy single H/P knockin mice (Figure 1C), neoplastic double H/P;A/E knockin spleen samples demonstrated complete recombination of the H/P allele, suggesting expansion of cells harboring the recombined allele (Figure 2C). Recombination of the H/P and A/E stop cassettes was also

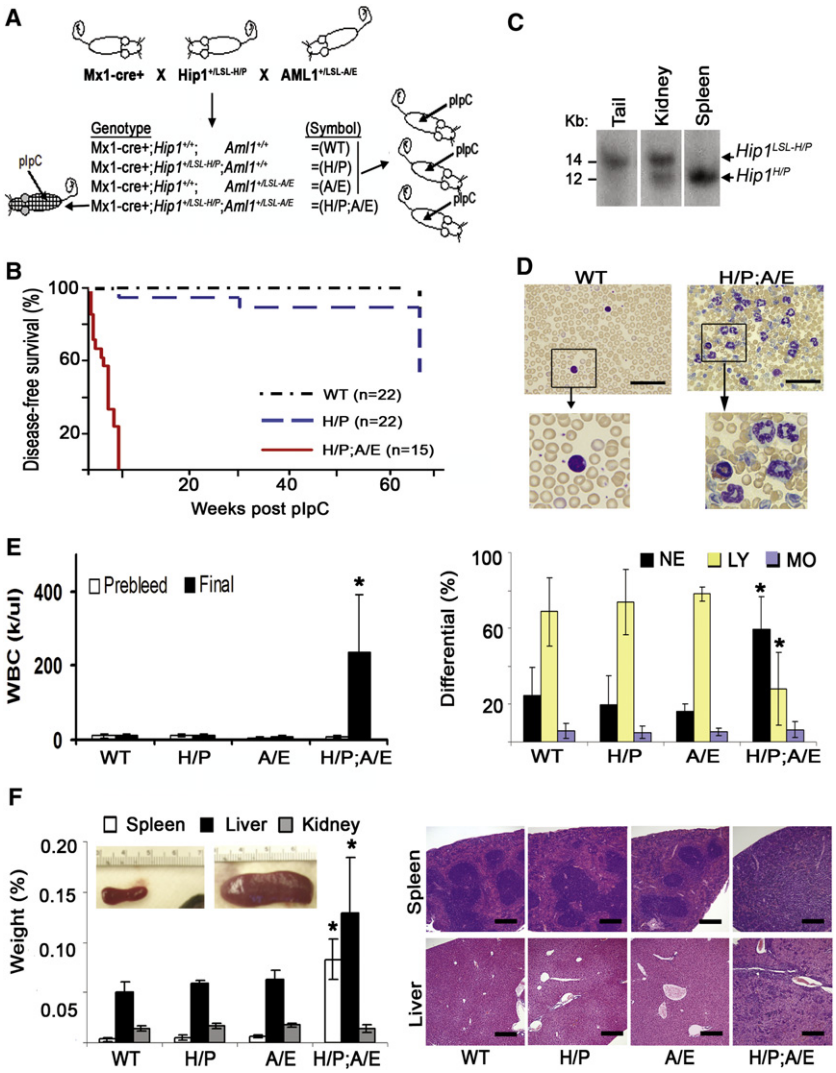

Figure 2. Expression of H/P;A/E Leads to a CML-like MPD

(A) Schematic of the mating scheme that was used to produce the double knockin mice used in this study. Also shown are the symbols used to designate the different genotypes.

(B) The Kaplan-Meier curve depicts disease-free survival as a function of time in weeks since pIpC induction. The rapid decline in disease-free survival of H/P mice at 67 weeks reflects occult abnormalities discovered at necropsy (Table 1).

(C) Southern blot analysis (cDNA probe) of EcoRV-digested DNA from multiple tissues from a pIpC-induced H/P;A/E mouse shows no recombination in the tail, partial recombination in the kidney, and complete recombination in a neoplastic spleen.

(D) Peripheral blood smears from control (WT) and diseased mice (H/P;A/E) are represented. Scale bar represents 40 μm.

(E) Complete blood counts (CBC) from wild-type (WT; n = 9), H/P (n = 11), A/E (n = 3), and H/P;A/E (n = 8) mice were determined prior to pIpC induction (prebleed) and then after pIpC induction once weekly to determine onset of disease. Average final WBCs at necropsy are displayed (left panel). H/P;A/E mice developed a severe myeloid leukocytosis (right panel; NE, neutrophil; LY, lymphs; MO, monocytes). Values are mean ± SD. Asterisk denotes a significant difference ($p < 0.01$) compared with WT mice.

(F) Massive hepatosplenomegaly in H/P;A/E mice. All livers and spleens (left inset is a WT spleen, and right inset is a H/P;A/E spleen) from H/P;A/E mice were greatly enlarged at necropsy while kidneys were normal (WT n = 9, H/P n = 11, A/E n = 3, H/P;A/E n = 8; mean ± SD; *$p < 0.01$). Histological analysis of hematoxylin and eosin-stained spleen and liver tissue from WT, H/P, A/E, or H/P;A/E mice were examined (right hand panels). Effacement of the normal follicular architecture of the spleen and infiltration of the liver was observed only in the H/P;A/E mice. Scale bar represents 300 μm.

detected in peripheral blood by PCR (data not shown). Bone marrow cells from diseased H/P;A/E mice readily grew under monocytic (or myeloid) culture conditions, and the H/P protein was detected in these cells by western blot (data not shown). These data indicate that simultaneous activation of the H/P and A/E oncogenes confers a selective growth advantage to hematopoietic cells.

We next examined the cellular characteristics of the spleen and bone marrow from wild-type, single knockin, or double knockin mice 4 weeks after pIpC induction to more thoroughly analyze the hematopoietic neoplasia. Spleen cellularity was sharply elevated in induced H/P;A/E mice (Figure 3A), whereas bone marrow cellularity was diminished (Figure 3B). In both tissues, the frequency of Mac-1$^+$Gr-1$^+$ myeloid cells was increased (Figures 3A and 3B, right hand panels). This expansion of differentiated myeloid cells was associated with a relative decrease in frequency of B, T, and erythroid cells in bone marrow and spleen (Figure S4 and data not shown). Although hematopoietic stem cell (HSC) frequency was reduced in the bone marrow of both the single H/P knockin mice and the H/P;A/E mice (Figure 3C, left hand panel), the absolute number of HSCs in the H/P;A/E spleen was increased (Figure 3C, right hand panel), consistent with the onset of extramedullary hematopoiesis, which often occurs in the context of hematopoietic malignancies. The diminished frequency of HSCs in the single H/P knockin mice was not observed in the 1.5-year old single H/P knockin mice (Table S2) and was therefore not pursued further for this study. In addition, the frequency of bone marrow cells that formed primitive GEMM colonies or GM colonies in methylcellulose was also reduced upon H/P;A/E induction (Figure 3D). Together, these cellular characteristics are consistent with the development of a CML-like MPD in induced H/P;A/E mice.

It is possible that the diminished bone marrow HSC frequency was due to an intrinsic effect of oncogene expression on HSC maintenance or due to an extrinsic effect of the leukemic cells on normal HSC survival (or both). To test these possibilities in the H/P;A/E-expressing mice, we conducted a competitive bone marrow repopulation experiment. In this experiment, 1,000,000 bone marrow cells from uninduced Mx1Cre;H/P;A/E or Cre negative control mice (CD45.2) together with 500,000 wild-type cells from recipient-type bone marrow (CD45.1) were used as donor cells (Figure 4A shows schematic). Recipients

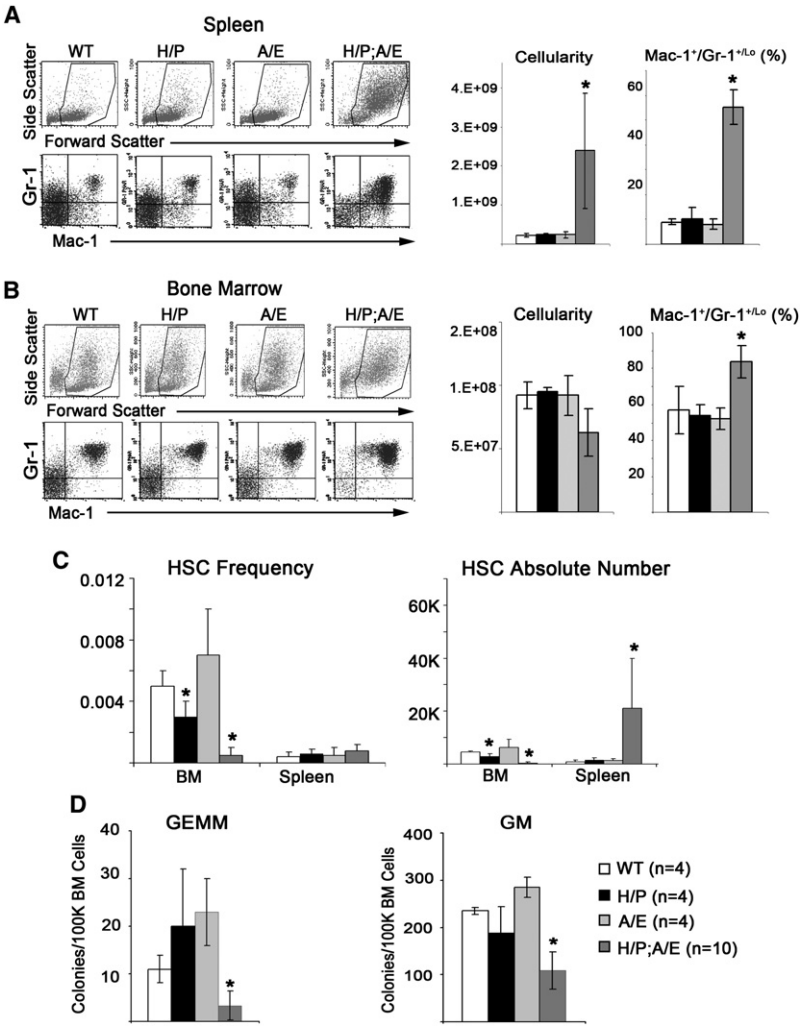

Figure 3. Abnormal Immunophenotype of Hematopoietic Cells from the Bone Marrow and Spleen of H/P;A/E Mice

(A, B) Single cell suspensions of bone marrow and spleen cells from pIpC-induced Mx1-Cre transgenic mice (average 3 weeks after induction) that were either WT, H/P, A/E, or H/P;A/E were analyzed by flow cytometry. Values in all the bar graphs are mean ± SD. Representative flow cytometry profile of forward and side scatter of spleen cells (A) and bone marrow cells (B). These profiles illustrate the presence of a distinct, uniform population of enlarged cells (box) in the spleen and bone marrow of H/P;A/E mice. Representative profile of the myeloid immunophenotype illustrates a significant increase in both mature granulocytic ($Gr1^+/Mac1^+$) and monocytic ($Gr1^{lo}/Mac1^+$) populations (A, B, left lower panels) in H/P;A/E mouse spleen and bone marrow. For WT (white bar), H/P (black bar), and A/E (light gray bar) mice, n = 4. For H/P;A/E (dark gray bar) mice, n = 10. Asterisk denotes a significant difference ($p < 0.01$) between H/P;A/E mice and WT, H/P, or A/E mice.

(C) The frequency (%) of $CD150^+CD48^-CD41^-Sca\text{-}1^+c\text{-}kit^+$ HSCs in the bone marrow of H/P;A/E (dark gray bars) mice was significantly reduced. Asterisk denotes a significant difference between H/P;A/E and WT mice ($p < 0.01$).

(D) The frequencies of CFU-GEMM and CFU-GM colonies were significantly diminished in the bone marrow from H/P;A/E mice (dark gray bar) compared with WT (white), H/P (black), or A/E (light gray) mice.

(CD45.1) were analyzed for stable peripheral blood chimerism 6 weeks after transplant and then induced with pIpC. As expected, all of the Mx1Cre;H/P;A/E recipients developed a CML-like MPD that was grossly and histologically identical to that of the primary mice (Figure S5). Two weeks after induction (during early stages of disease), groups of mice from Mx1Cre; H/P;A/E and control transplants were euthanized, and their bone marrows were analyzed for HSC distribution (n = 3 each group). For both groups, HSCs were distributed in the expected 2:1 ratio of CD45.2 donor-type to CD45.1 recipient-type (Figure 4B). However, the total numbers of recipient *and* donor-type HSCs were significantly decreased in the Mx1Cre+;H/P;A/E recipients compared with Cre-negative controls (Figure 4C). Together, these data indicate the presence of an extrinsic inhibitory effect of the H/P;A/E-expressing CML-like MPD on the HSC compartment.

We next attempted to transplant the CML-like MPD from H/P; A/E mice into secondary recipients. The direct transfer of unfractionated primary neoplastic cells from diseased H/P;A/E mice to immunocompromised or syngeneic recipient mice was highly inefficient, consistent with prior studies that have found MPDs relatively difficult to transplant (Kogan et al., 2002; Lee et al., 2007; Sirard et al., 1996). For example, when sublethally irradiated (1 × 240 rad), NOD/SCID-IL2Rγ mice were retro-orbitally injected with unfractionated bone marrow cells (2×10^6) from H/P knockin, A/E knockin, or diseased double H/P;A/E knockin animals. None of the recipients displayed evidence of disease for up to 20 weeks (data not shown). In lethally irradiated syngeneic CD45.1 recipients, up to 6×10^6 whole bone marrow cells from multiple diseased donors (n = 4) were also highly inefficient at transplanting the disease (Table 2, "vehicle"). Similar results were obtained with unfractionated splenocytes. The relative inability of cells from animals with H/P;A/E-induced disease to transfer disease upon transplantation is consistent with the idea that the vast majority of CML cells have a limited capacity to proliferate (Kavalerchik et al., 2008; Savona and Talpaz, 2008; Sawyers et al., 1992). Furthermore, these data also support the categorization of this hematopoietic neoplasia as a CML-like MPD rather than a transplantable leukemia (Kogan et al., 2002).

To begin to identify the LIC from the diseased mice, we performed transplant experiments with FACS-purified HSCs. Although transplantation of HSCs from these mice did not transfer a florid CML-like MPD into syngeneic recipients, these cell transfers resulted in rapid death after transplant in a high frequency of recipients (Table 2). This was despite the fact that sufficient "radio-protective" bone marrow cells were mixed with the purified HSCs for transplant success. Histological analysis of the spleens from the mice that received the purified HSC transplantation demonstrated myeloid infiltrates that were consistent with an MPD. The inability to transfer a full blown

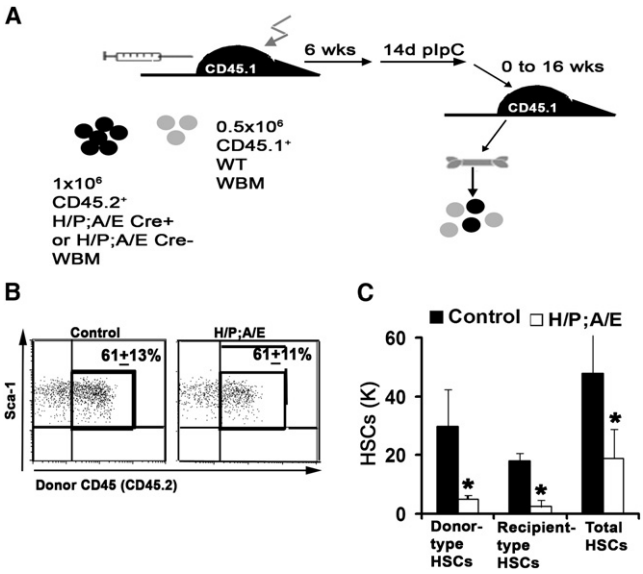

Figure 4. Although an H/P;A/E-Expressing MPD Results from an Intrinsic Transforming Effect, There Is an Extrinsic Inhibitory Effect on Normal BM HSC Frequency

(A) Irradiated (CD45.1) recipients were transplanted with twice as many donor (CD45.2) Mx1-Cre;H/P;A/E or control bone marrow cells to recipient (CD45.1) bone marrow cells. Six weeks after transplantation, recipient mice were treated with pIpC for 2 weeks to induce recombination. Mice were bled 4 weeks after induction to monitor disease progression. All of the mice transplanted with the Mx1-Cre;H/P;A/E bone marrow were with splenomegaly and leukocytosis similar to the primary disease, whereas the H/P;A/E Cre negative donors were disease free (Figure S5).

(B) Cells from bone marrow 4 weeks after pIpC induction were analyzed for frequency of $CD150^+CD48^-CD41^-Sca\text{-}1^+c\text{-}kit^+$ (SLAM HSCs) donor versus recipient cells. The donor cells accounted for 61% of HSCs in recipient mice as expected, whether the mice had been transplanted with control donor cells or H/P;A/E donor cells. Values represent mean ± SD of three mice per treatment.

(C) The absolute number of both donor-type (H/P;A/E) and recipient-type (WT) bone marrow HSCs decreased significantly in HP/AE recipients when compared with control recipients. The total number of HSCs (donor-type + recipient-type) was also drastically reduced. Values represent mean ± SD of three mice per treatment. Asterisk denotes a significant difference ($p < 0.05$) compared with control recipients.

hematopoietic neoplasia to wild-type recipients with these cells is consistent with the presence of an extrinsic inhibitory effect of the diseased cells on normal cell hematopoiesis (Figure 4C). These data also suggest that tumorigenic cells (or LICs) from the diseased H/P;A/E mice might be present in the phenotypic HSC fraction.

Imatinib Treatment Reduces Leukemic Burden, but Not LICs

To determine whether PDGFβR signaling from H/P was critical to the maintenance of the H/P;A/E-induced neoplasia, a group of diseased mice were treated with imatinib or vehicle for 10–12 days by intraperitoneal injection (n = 4 imatinib, n = 3 vehicle). All vehicle-treated H/P;A/E-induced mice exhibited progressive hepatosplenomegaly, effacement of splenic architecture, and myeloid infiltration of their livers and lungs. Imatinib therapy did not appear to exert any discernible effects on wild-type animals

Table 2. Imatinib Does Not Eliminate LICs from H/P;A/E CML-like Disease

Donor Cell No.	Treatment[a]	Donor N	Recipients with Disease[b] Diseased/Total (%)
Whole Bone Marrow (WBM) Transplants			
100,000	Vehicle	2	1/8 (12%)
500,000	Vehicle	2	0/10 (0%)
2,000,000	Vehicle	3	1/14 (7%)
6,000,000	Vehicle	2	0/8 (0%)
100,000	Imatinib	3	3/14 (21%)
500,000	Imatinib	3	5/14 (36%)
2,000,000	Imatinib	3	7/13 (54%)
Hematopoietic Stem Cell (HSC) Transplants			
50	Vehicle	1	1/5 (20%)
10	Vehicle	1	3/5 (60%)
5	No Rx	1	1/7 (14%)
50	Imatinib	1	5/5 (100%)
10	Imatinib	1	5/5 (100%)

[a] H/P;A/E CML-like diseased mice were treated for 10–14 days with imatinib or vehicle prior to transplant of their bone marrow cells into lethally irradiated syngeneic recipient mice. WBM or FACS isolated HSCs were cotransplanted with 200–400,000 wild-type bone marrow cells.

[b] Fraction of recipients with overt CML-like MPD or rapid death after transplant. All of the HSC transplanted mice died rapidly after transplant and were found to have evidence of an MPD.

(data not shown). In contrast, imatinib treatment of H/P;A/E-induced mice led to a rapid response as evidenced by reduction of WBCs to wild-type levels ($p = 0.01$, Figure 5A). Upon necropsy, significant decreases in spleen ($p = 0.0005$) and liver ($p = 0.004$) size were also observed (Figure 5B and data not shown). Histologically, splenic architecture was normalizing, and the liver appeared free of myeloid infiltrates (Figure 5C). This rapid hematological response to imatinib is consistent with that observed following imatinib treatment in humans with CML (Savona and Talpaz, 2008) and in mice with retroviral expression of tyrosine kinases such as BCR/ABL (Wolff and Ilaria, 2001) and TEL/PDGFβR (Grisolano et al., 2003).

We next analyzed the effect of imatinib on HSC frequency in H/P;A/E mice. Compared with vehicle-treated mice, bone marrow from imatinib-treated mice displayed a restoration of nearly normal HSC frequency in bone marrow (0.0026 ± 0.0018, $p = 0.05$; Figure 5D and data not shown). Interestingly, in contrast to the reduction observed in spleen cellularity, bone marrow cellularity was not immediately restored, presumably due to the depletion of CML-like MPD cells from the bone marrow (Figure 5B). The increase in bone marrow HSC numbers concomitant with the depletion of neoplastic cells suggests the presence of a differential effect of imatinib on bulk tumor cells as compared to HSCs.

In order to begin to determine whether imatinib affected the frequency of LICs, we transplanted unfractionated bone marrow from vehicle- or imatinib-treated H/P;A/E mice into lethally irradiated syngeneic recipients along with a radioprotective dose of 200,000 wild-type bone marrow cells. We predicted that imatinib therapy would eliminate the limited transplantability of unfractionated bone marrow. Transplants were performed after 10–12 days of imatinib therapy, when imatinib-treated mice displayed

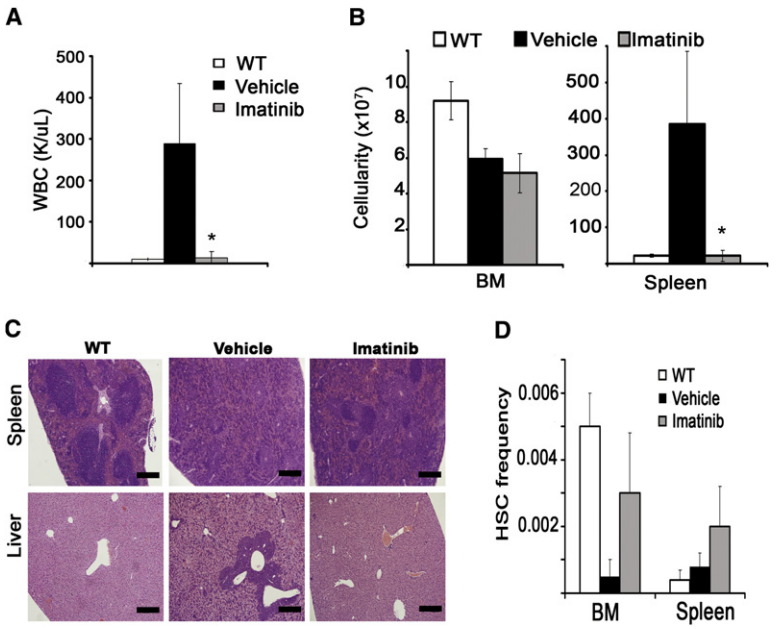

Figure 5. Imatinib Treatment Eliminates the Bulk of the Neoplasia

Values in all the bar graphs are mean ± SD.

(A) Imatinib normalized WBCs after 10 days of treatment (*p = 0.01, vehicle versus imatinib).

(B) Imatinib-treated mice exhibited markedly reduced spleen cellularity (*p = 0.01, vehicle versus imatinib), but bone marrow cellularity was not immediately normalized.

(C) Imatinib treatment began to restore splenic architecture and cleared myeloid infiltrates from the liver. Scale bar represents 300 μm.

(D) The frequency (%) of HSCs was partially rescued in the bone marrow (p = 0.05, imatinib versus vehicle) but not in the spleen. Splenic HSC frequency was increased in imatinib-treated mice (presumably because leukemic burden was dramatically reduced, increasing the frequency of normal HSCs in the spleen), but the difference was not statistically significant. +/+ indicates untreated wild-type mice (n = 7); vehicle, vehicle-treated pIpC-induced H/P;A/E mice (n = 3); imatinib, imatinib-treated pIpC-induced H/P;A/E mice (n = 4).

normalized WBC counts. Regardless of the transferred cell number, bone marrow cells and splenocytes from imatinib-treated mice were consistently *more* likely to transfer disease than cells from vehicle-treated mice (Figure 6A, Tables 2 and S3). The recipient disease was grossly and histologically similar to that in the donors, and no recipients showed evidence of progression to accelerated or blast crisis phases of the disease (Figure 6B). The disease in recipient mice remained hematologically sensitive to imatinib therapy (Figure 6B), indicating that the transferred cells did not represent imatinib-resistant clones from the donor animals. The increased transplantability of bone marrow LICs in H/P;A/E mice after imatinib treatment contrasted dramatically with the reduced neoplastic burden in these mice and suggested that LICs are less sensitive to imatinib than other neoplastic cells of the MPD. Further evidence for this refractoriness of the LICs was accumulated when a rapid return of the MPD disease state was observed following withdrawal of imatinib from H/P;A/E-expressing mice that were put into remission with imatinib therapy (data not shown). For example, we have continuously treated H/P;A/E mice for up to 26 days with imatinib and found that upon withdrawal of imatinib we have observed a return of disease.

Clear differences in long-term multilineage reconstitution activity were also evident between recipients of vehicle- and imatinib-treated bone marrow samples (Figure 6C). Only 60% of recipients of vehicle-treated bone marrow cells showed long-term multilineage reconstitution by donor cells, confirming the decrease in HSC frequency in untreated, induced H/P;A/E mice (Figures 3C and 5D). In contrast, almost all recipients of bone marrow cells from imatinib-treated mice showed long-term multilineage reconstitution (Figure 6C). This correlation of increased functional HSC activity (reconstitution) with the increased transplantability of the MPD in imatinib-treated mice is additional evidence (to the HSC transplant data) that the LIC is contained in the HSC fraction.

Although we have not yet definitively purified the LIC in these mice, the evidence thus far indicates that LICs might be found in the HSC compartment and are relatively refractory to imatinib. Interestingly, FACS-isolated HSCs from imatinib-treated mice upon transplantation into irradiated mice more frequently led to early lethality with an MPD compared with HSCs from vehicle-treated mice (Table 2), suggesting that the increased bone marrow transplantability observed in the imatinib-treated mice (Figure 6) might not just induce a change in LIC frequency but might also modulate their tumorigenicity.

A few possible mechanisms for how the LICs might be insensitive to imatinib while the bulk tumor cells readily respond to imatinib include the following: lack of H/P kinase inhibition in LICs due to low intracellular levels of imatinib despite high doses of drug delivered, lack of expression of the H/P protein in the LICs despite recombination, extremely high levels of H/P expression that overwhelm "therapeutic" levels of the drug, or lack of addiction of these cells to H/P due to quiescence or other unknown "context" factors. We have gathered some evidence that indicates that H/P-expressing cancer cells may or may not be addicted to H/P signaling depending on the milieu they are in. For example, H/P-expressing Ba/F3 cells (similar to BCR/ABL-expressing Ba/F3 cells) are sensitive to imatinib ("addicted") in the absence of IL-3; however, when IL-3 is present, the survival of these cells in the presence of imatinib is no different than wild-type Ba/F3 cells (Figure S6). In this case we know that the H/P protein is expressed in the cells in the presence or absence of IL-3 so the relative resistance is not due to lack of H/P expression and instead is due to IL-3 induced environmental changes that cure the cells of their H/P addiction. Until we are able to purify enough LICs from H/P;A/E-expressing mice to characterize them, the precise mechanism of their imatinib refractoriness in vivo remains to be determined and the above list of possibilities comprise only a subset of avenues for future investigation of this complex issue.

DISCUSSION

The role of activating mutations of receptor tyrosine kinases (RTKs) in hematopoietic malignancies is well-established.

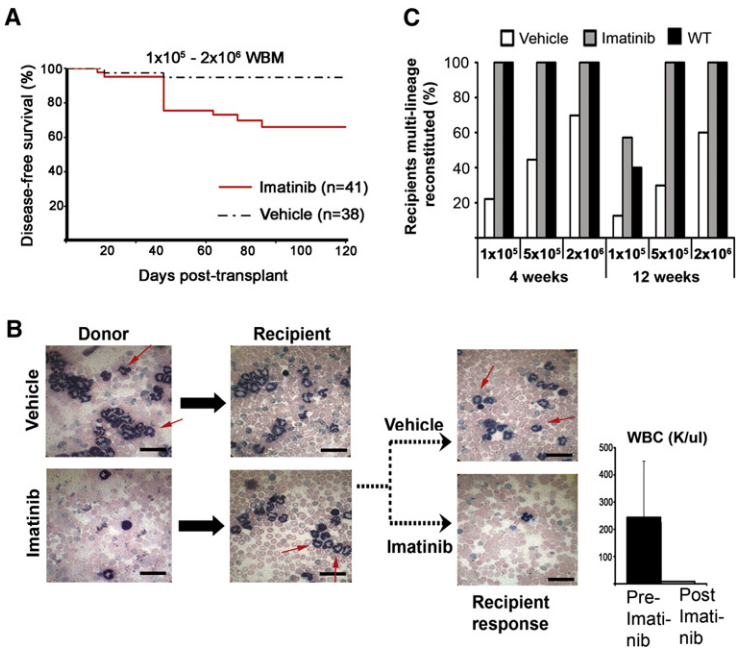

Figure 6. Imatinib Treatment Rescues HSC Activity but Also Increases the Frequency of LICs

(A) Graded doses of 1 × 10^5 to 2 × 10^6 whole bone marrow cells (WBM) from pIpC-induced H/P;A/E CD45.2 mice that were treated with vehicle (n = 4 donors, 38 recipients) or imatinib (n = 3 donors, 40 recipients) for 7–10 days were transplanted into lethally irradiated CD45.1 recipients along with 2 × 10^5 wild-type CD45.1 bone marrow cells. Recipients of bone marrow cells from imatinib-treated mice developed CML at a greater frequency than recipients of vehicle-treated bone marrow cells.

(B) Representative peripheral blood smears of pIpC-induced H/P; A/E donor mice treated with vehicle displayed an abundance of mature granulocytes (upper left, arrows), which were greatly reduced in imatinib-treated mice (lower left). This CML-like MPD was transplantable, with some recipients of vehicle- (middle, top) and imatinib-treated (middle, bottom) WBM developing a similar disease. Note the predominantly mature granulocytic cells in the bottom panels and the absence of blasts. The primary mice that were treated with imatinib displayed the most transplantable disease and the disease remained sensitive to imatinib treatment (right hand panels). Scale bar represents 30 μm. Values in all the bar graphs are mean ± SD.

(C) WBM from imatinib-treated mice more frequently gave rise to multilineage reconstitution (donor myeloid, B, and T cells) at 12 weeks after transplantation compared with vehicle-treated mice (at 4 weeks: n = 29 for vehicle, n = 27 for imatinib; at 12 weeks: n = 27 for vehicle, n = 18 for imatinib). Reconstitution was defined as the presence of greater than 0.3% donor type CD45.1 marker in B (B220), T (CD3), and myeloid (Mac1, Gr1) lineages. Black bars indicate multilineage reconstitution of Cre-negative H/P;A/E (control) bone marrow recipients (n = 15).

PDGFβR is one such RTK that is a frequent target in myeloid leukemias. More than 15 different translocations have been identified in human CMML patients that lead to constitutively active fusion variants of PDGFβR (Curtis et al., 2007). Accumulating evidence suggests that all PDGFβR-containing translocations share many properties and are functionally interchangeable. For example, one such translocation, t(5;7)(q33;q11.2), fuses the majority of the *HIP1* gene to the transmembrane and catalytic domains of the *PDGFβR* gene (Ross et al., 1998). Like all of the other PDGFβR fusions, the H/P fusion protein is a constitutively active tyrosine kinase that is able to transform hematopoietic cells to factor-independent growth in culture (Ross et al., 1998) and activate the PI3K, MapK, PLC-gamma and STAT5 pathways (Ross and Gilliland, 1999). The role of these oncogenes in vivo has only been studied using the retroviral bone marrow transduction and transplantation assays. In the current study, we employed a previously described knockin strategy (Higuchi et al., 2002) that couples a *loxP* bracketed transcriptional stop cassette with an inducible Cre transgene to generate a mouse in which lineage-specific expression of H/P can be temporally and spatially controlled. This strategy allows us to bypass any embryonic lethality that results from the expression of H/P (Oravecz-Wilson et al., 2004) and to directly determine the development of disease in the adult mouse in the presence or absence of other genetic lesions such as a conditional A/E knockin allele (Higuchi et al., 2002).

Following the generation of the *Mx1-Cre;Hip1*$^{+/LSL\text{-}H/P}$ mice, we found that these mice did not frequently develop hematopoietic malignancies following pIpC induction even after 1.5 years. H/P expression is, therefore, not sufficient to cause cancer, though a minority of mice did exhibit enlarged spleens and liver tumors, suggesting that H/P expression increases the risk of carcinogenesis. This finding contrasts starkly with BTT assays where retroviral expression of tyrosine kinase oncogenes such as H/P (Figure S1), TEL/PDGFβR (Grisolano et al., 2003), and BCR/ABL (Neering et al., 2007) induced a MPD similar to CML. Importantly, because healthy, nonneoplastic tissues (kidney, liver, spleen) from pIpC-treated *Mx1-Cre;Hip1*$^{+/LSL\text{-}H/P}$ mice maintained *Hip1*$^{H/P}$ alleles (Figure 1G), the possibility that *Hip1*$^{H/P}$-containing cells were selected against over time is an unlikely explanation for the lack of disease after 1.5 years. Because use of endogenous regulatory elements to express the H/P oncogene did not lead to the MPD observed following retroviral expression of tyrosine kinase oncogenes, the cell type and/or oncogene levels are seemingly key variables to control when developing mouse models of human cancers.

In contrast to the finding that expression of H/P alone did not result in transformation of hematopoietic cells in vivo, coinduction of H/P with A/E led to a florid MPD within days of induction. Thus, contrary to the BTT models of tyrosine kinase oncogene and A/E oncogene cooperation that yield longer disease latency and predominantly acute leukemia (Grisolano et al., 2003; Schessl et al., 2005), this murine model provides direct evidence that expression of A/E in adult myeloid progenitors in vivo does not completely block differentiation but instead cooperates with H/P to induce an explosive myeloproliferative neoplasm. Moreover, these data confirm that A/E-induced leukemia is a multistep process, in which secondary genetic alterations, such as H/P fusion protein generation, cooperate with A/E to induce full transformation. This report demonstrates that a human oncogene can indeed cooperate with the A/E knockin allele to produce transformation (Higuchi et al., 2002).

Although a clear hematologic response to imatinib was observed in these double knockin mice, transplant and drug

withdrawal experiments demonstrated that LICs were not eliminated by this therapy. This H/P;A/E disease model highlights the need for therapies that not only target oncoproteins but also preferentially kill leukemogenic cells. The mechanism(s) of resistance of LICs to imatinib therapy is not yet understood, but possibilities such as limited intracellular drug levels in the LIC, limited expression of the oncogene, relative quiescence, or lack of addiction of the LIC to the oncogene are all currently under investigation. It will be important to determine if the LICs depend upon the initiating H/P oncogene signals for survival. If the LIC is not dependent upon, or cannot be manipulated to be dependent upon, the H/P activity, then therapeutic variations on the imatinib therapy theme will be ineffective.

These mice model the neoplastic role of the growing family of PDGFβR human translocations in vivo more accurately than before by using a conditional knockin technology. Furthermore, these experiments provided intriguing insights into how the different ways used to model leukemia in mice influence outcomes and conclusions. We expected that activation of a single copy of H/P cDNA knocked into the endogenous *Hip1* locus in the adult mouse would be sufficient to induce a chronic MPD. In addition, based on the report by Grisolano et al. (2003), we expected that coinduction of A/E with this H/P allele would result in an increased frequency or severity of the H/P-induced disease and would inhibit myeloid differentiation leading to acute leukemia. To our surprise, however, a very low frequency of neoplasia was observed in the single H/P knockin mice, and a shockingly high frequency (100% penetrance) and an essentially absent disease latency of an explosive MPD (rather than acute leukemia) was observed in the double knockin mice. This observation directly counters the prevailing idea that A/E functions via prevention of hematopoietic differentiation (Reilly, 2003). If this notion were true, the H/P;A/E knockin mice would be immediately blastic and have impaired differentiation. These findings raise the possibility that modeling leukemogenic events under the most genetically realistic conditions might help us identify environmental or genetic triggers that lead to the development of CML accelerated phase or frank blast crisis.

In sum, the conditional activation of H/P in the hematopoietic system of adult mice leads to an explosive, mature, imatinib-sensitive MPD when coexpressed with A/E. Importantly, LIC activity was persistent in induced H/P;A/E mice following imatinib treatment because their bone marrow was able to transplant this imatinib-sensitive MPD more readily than vehicle-treated mice. This model will therefore serve as an invaluable tool for in-depth studies of the therapeutic effect of PDGFβR (imatinib, MAPK inhibitors, rapamycin) and A/E (trichostatin A, SAHA) inhibitors as well as allow for further rigorous in vivo characterization of the cellular and molecular mechanisms of hematopoietic transformation and drug resistance.

EXPERIMENTAL PROCEDURES

Generation of Conditional H/P Knockin Mice

The conditional H/P knockin allele, *Hip1*$^{LSL\text{-}H/P}$, was generated by modifying the original H/P knockin target vector that contained a human H/P cDNA in frame with murine *Hip1* exon 2 (Oravecz-Wilson et al., 2004). Two custom vectors were constructed with desired multiple cloning sites (designated AMP1 with *Spe*I, *Eag*I, EcoRI, *Not*I/*Eag*I, BamHI, and SalI sites; and AMP2 with *Not*I, KpnI, HindIII, and SalI sites). The 5′ *Not*I/BamHI 8.2 kb fragment from the original H/P knockin vector was subcloned into the *Eag*I/BamHI sites of AMP1 and named N/B7+KI. Subsequently, the *Spe*I/EcoRI 7.2 kb fragment from N/B7+KI was ligated into the EcoRI/EcoRI 4 kb subclone from the original HIP1/PDGFR knockin target vector and into the AMP1 vector digested with *Spe*I and EcoRI (named p1N/RI/RI 5′). Next, a 1.5 kb DNA fragment containing a transcription termination stop cassette flanked by *loxP* sites was inserted, as an AscI cassette, 5′ to the HIP1/PDGFR cDNA into the KpnI site of HIP1's intron 2 (KpnI site modified to *Asc*I by the paired oligos: 5′-AACATTGGCGCGCC ACAAGTCGTAC-3′ and 5′-GACTTGTGGCGCGCCAATGTTGTAC-3′) and designated as p1N/RI/RI 5′ stop. This stop cassette contains the SV40 polyadenylation signal, thus preventing full-length transcripts from being made until the stop cassette is removed by Cre recombinase. In addition, an ATG translation start site and 5′ splice donor are encoded to prevent correct expression of the HIP1/PDGFR fusion due to downstream transcription. The 3′ half of the target vector was constructed in the AMP2 vector by first subcloning the 4 kb HIP1 exon 6 and 7 Hind H/B subclone into the HindIII site of AMP2 (designated p2H4). A PGK-neomycin *Not*I/KpnI cassette lacking *loxP* sites was generated by PCR using the original target vector as a template and the following primers: 5′-TTTGCGGCCGCTAGGTCTGAAGAGGAGTTTAC-3′ and 5′-TTTGGTACC ATTAAGGGTTCCGGATCGATC-3′. This *Not*I/KpnI neo PCR product was subcloned into p2H4 5′ of the HIP1 genomic DNA (named p3H4neo). The final conditional H/P knockin target vector was generated by subcloning the p3H4neo *Not*I/SalI 5.5-kb fragment into the corresponding sites in p1N/RI/RI5′ stop so as to fuse the neomycin resistance cassette and HIP1 3′ genomic DNA to the 3′ end of the polyadenylation signal for the H/P cDNA. The final targeting vector was ~21.5 kb. Electroporation into ES cells and screening by Southern blot for clones that were correctly targeted with the 3′ genomic probe was performed as described (Oravecz-Wilson et al., 2004).

Southern Blot Analysis

Southern blot analysis to distinguish the targeted *Hip1*$^{LSL\text{-}H/P}$ allele and the wild-type allele was performed with the 3′ probe as described for the *Hip1*^{null} allele (Oravecz-Wilson et al., 2004). For recombination of the targeted allele, a hHIP1 cDNA probe ("5′ probe" encompassing HIP1 sequences up to the internal EcoRI site [nt 1260]; Figure 1) was used under the same conditions as those used for the 3′ genomic probe.

Double and Triple Transgenic Mice

Double transgenic Mx1-Cre;*Hip1*$^{+/LSL\text{-}H/P}$ mice were generated by crossing the *Hip1*$^{+/LSL\text{-}H/P}$ mice with mice transgenic for the Mx1-Cre gene (obtained from Jackson Labs [Kuhn et al., 1995]). Triple transgenic Mx1-Cre;*Hip1*$^{+/LSL\text{-}H/P}$; *Aml1*$^{+/LSL\text{-}A/E}$ mice were generated by crossing the Mx1-Cre;*Hip1*$^{+/LSL\text{-}H/P}$ mice with *Aml1*$^{+/LSL\text{-}A/E}$ mice (Higuchi et al., 2002). Expression of Cre recombinase was induced by injecting mice intraperitoneally with 250 μg pIpC (Sigma, St. Louis, MO) in 100 ul PBS at 2-day intervals for 2 weeks as previously described (Yilmaz et al., 2006). For this study, a total of 69 triple transgenic mice were generated and 17 (25%) had spontaneous recombination due to endogenous interferon mediated Mx1-Cre activation. We conclude this because double knockin mice that were Mx1-Cre negative never underwent recombination. Mice were mated onto a C57Bl/6 genetic background. Mice were housed in the Unit for Laboratory Animal Medicine at the University of Michigan under specific pathogen-free conditions and were monitored regularly for evidence of disease and abnormal peripheral blood cell counts. All mouse experiments were conducted after approval by the University of Michigan Committee on Use and Care of Animals.

Hematopoietic Analysis

Induced cohorts of 22 Mx1Cre; *Hip1*$^{+/LSL\text{-}H/P}$ and 23 Mx1Cre; *Hip1*$^{+/+}$ littermate animals were bled on a monthly basis for determination of CBCs. Numbers were pooled from each time point. Induced double H/P;A/E knockin mice were bled on a weekly basis. Blood was collected into a tube containing EDTA (Sarstad) and analyzed with an 850 HEMA-VET machine (CDC Technologies).

For the time course of peripheral smears (Figure 2SC) from the double knockin mice, mice were prebled by submandibular bleed prior to treatment with pIpC. Twenty-four hours after treatment, daily tail bleeds were initiated. Smears were stained with Wright-Giemsa.

Flow cytometric analysis, methylcellulose assays, and quantitation of HSCs from bone marrow and spleen were performed as described previously (Yilmaz et al., 2006). The total number of $CD150^+CD48^-CD41^-Sca\text{-}1^+c\text{-}kit^+$ cells (HSCs) per mouse was calculated based on the frequency of this population in the bone marrow and spleen, the cellularity of the spleen and long bones, and the assumption that 15% of all bone marrow is within the long bones. Blood and other tissues do not contribute significantly to the overall size of the HSC pool.

PCR Genotyping

Mouse tail DNA was used for PCR detection of the various germ line alleles. *Hip1*$^{LSL\text{-}H/P}$ specific primers were 5′EcoRI (5′-CTGAGAGCCAGCGGGTTGT GCTGCAGCTGA-3′) and 3′EcoR1 (5′-CTCCTTTAGCTTGCTATATCGCTGTT CATTGGC-3′). Cre allele primers were IMR567 (5′-ACCAGCCAGCTATC AACTCG-3′) and IMR568 (5′-TTACATTGGTCCAGCCACC-3′). Aml1 primers were Int3.up (5′-ATCAAATGATGACGACGG-3′), Ex5.low (5′-TGATGGCTCTA TGGTAGGTGG-3′), and Int4.low (5′-CAGTTTAGGAAAACGGTGG-3′). The expected product sizes for *Hip1*$^{LSL\text{-}H/P}$ and Cre products were 200 base pairs. The Aml1 expected product (Int3.up and Int4.low primer pair) was 596 base pairs and, the A/E knockin product was 378 base pairs (Ex5.low and Int4.low primer pair). Pretreatment of 2 μl (100 ng/μl; 200 μg total) of DNA with 5 μl gene releaser (Bioventrue) was performed.

PCR analysis for *Hip1*$^{LSL\text{-}H/P}$ recombination to *Hip1*$^{H/P}$ (Figure 1G) was performed as follows. Genomic DNA was isolated from lysed peripheral blood samples or organs using standard protocols. Recombination of the floxed stop cassette was detected with the following primers: 5′-CTATCCAAGG GACCTGATGG-3′ and 5′-GCCAGTCCAAGGTGGATTTA-3′. The PCR conditions were as follows: 7 min at 94°C, 35 cycles of (30 s at 94°C, 1 min at 55°C, 1 min at 72°C), and 7 min at 72°C. The predicted recombined product was 336 base pairs, whereas the wild-type product was predicted at 200 base pairs. The nonrecombined product, which contained the entire stop cassette, was 2 kilobases and not amplified under these conditions. PCR analysis for A/E recombination was performed as described previously (Higuchi et al., 2002).

Histologic Analysis

Tissue obtained at necropsy was fixed in 10% formalin/PBS. Paraffin embedding and standard hematoxylin and eosin staining were performed by the University of Michigan Cancer Center Histology Core or Histoserv. MPO staining was carried out on deparaffinized and hydrated sections (xylene followed by 100%–50% EtOH). Antigen was retrieved with citrate buffer followed by incubation of the slide with 10% goat serum block and primary antibody (polyclonal anti-MPO, Abcam). Slides were blocked for endogenous peroxidase with 0.3% peroxide. The secondary antibody was biotinylated goat anti-rabbit (1:200, Jackson Immuno Research). The signal was amplified using the ABC kit (Pierce) and visualized with the DAB kit (Vector Labs). TUNEL assay was performed using the In Situ Cell Death Detection Kit (Roche), and nonspecific esterase staining was achieved with the nonspecific esterase staining kit (Sigma) following the manufacturer's instructions.

Imatinib Experiments

For the mouse treatment experiments, imatinib mesylate capsules (Novartis, 100 mg) were crushed and dissolved in sterile PBS with 10% DMSO at a final concentration of 20 mg/ml. The solution was filtered through a 0.1 uM syringe tip filter (Millipore). Mice were injected intraperitoneally once daily with 100 mg/kg. Mice were treated in pairs (vehicle or imatinib) until a complete hematologic response (normalized WBC) was observed in the imatinib-treated mouse (7–10 days), and then both the vehicle and imatinib-treated mice bone marrow was transplanted into irradiated syngeneic lethally irradiated Ly5.2 recipient mice as described previously (Yilmaz et al., 2006).

ENU Mutagenesis

Seven- to eleven-week-old Mx1-Cre-positive H/P or wild-type mice were intraperitoneally injected six times with 250 μg pIpC at 2 day intervals. Mice were then subcutaneously injected with four doses of 1 μg G-CSF followed by a single IP dose of 50 mg/kg ENU as described previously (Higuchi et al., 2002). Mice were then observed for disease for 11 months.

SUPPLEMENTAL DATA

Supplemental Data include six figures and three tables and can be found with this article online at http//www.cell.com/cancer-cell/supplemental/S1535-6108(09)00181-0.

ACKNOWLEDGMENTS

We thank Staelle Chamaillard and Jennetta Hammond for their technical assistance and the Ross lab members for their constructive intellectual input and for critical review of this manuscript. This work was supported by the National Cancer Institute grants CBTG CA009676 (S.T.P.), R01 CA82363-03 (T.S.R.), and R01 CA098730-01 (T.S.R.), a Burroughs Wellcome Fund Clinical Scientist Award in Translational Research (T.S.R.), and the Howard Hughes Medical Institute (S.J.M.). T.S.R. is a Leukemia and Lymphoma Society Scholar.

Received: October 3, 2008
Revised: March 21, 2009
Accepted: June 2, 2009
Published: August 3, 2009

REFERENCES

Breuer, M., Wientjens, E., Verbeek, S., Slebos, R., and Berns, A. (1991). Carcinogen-induced lymphomagenesis in pim-1 transgenic mice: dose dependence and involvement of myc and ras. Cancer Res. *51*, 958–963.

Cano, F., Drynan, L.F., Pannell, R., and Rabbitts, T.H. (2008). Leukaemia lineage specification caused by cell-specific Mll-Enl translocations. Oncogene *27*, 1945–1950.

Chen, W., Kumar, A.R., Hudson, W.A., Li, Q., Wu, B., Staggs, R.A., Lund, E.A., Sam, T.N., and Kersey, J.H. (2008). Malignant transformation initiated by Mll-AF9: gene dosage and critical target cells. Cancer Cell *13*, 432–440.

Curtis, C.E., Grand, F.H., Waghorn, K., Sahoo, T.P., George, J., and Cross, N.C. (2007). A novel ETV6-PDGFRB fusion transcript missed by standard screening in a patient with an imatinib responsive chronic myeloproliferative disease. Leukemia *21*, 1839–1841.

Druker, B.J., Guilhot, F., O'Brien, S.G., Gathmann, I., Kantarjian, H., Gattermann, N., Deininger, M.W., Silver, R.T., Goldman, J.M., Stone, R.M., et al. (2006). Five-year follow-up of patients receiving imatinib for chronic myeloid leukemia. N. Engl. J. Med. *355*, 2408–2417.

Gilliland, D.G. (2002). Molecular genetics of human leukemias: new insights into therapy. Semin. Hematol. *39*, 6–11.

Golub, T.R., Barker, G.F., Lovett, M., and Gilliland, D.G. (1994). Fusion of PDGF receptor beta to a novel ets-like gene, tel, in chronic myelomonocytic leukemia with t(5;12) chromosomal translocation. Cell *77*, 307–316.

Grand, F.H., Burgstaller, S., Kuhr, T., Baxter, E.J., Webersinke, G., Thaler, J., Chase, A.J., and Cross, N.C. (2004). p53-Binding protein 1 is fused to the platelet-derived growth factor receptor beta in a patient with a t(5;15)(q33;q22) and an imatinib-responsive eosinophilic myeloproliferative disorder. Cancer Res. *64*, 7216–7219.

Grisolano, J.L., O'Neal, J., Cain, J., and Tomasson, M.H. (2003). An activated receptor tyrosine kinase, TEL/PDGFbetaR, cooperates with AML1/ETO to induce acute myeloid leukemia in mice. Proc. Natl. Acad. Sci. USA *100*, 9506–9511.

Higuchi, M., O'Brien, D., Kumaravelu, P., Lenny, N., Yeoh, E.J., and Downing, J.R. (2002). Expression of a conditional AML1-ETO oncogene bypasses embryonic lethality and establishes a murine model of human t(8;21) acute myeloid leukemia. Cancer Cell *1*, 63–74.

Huettner, C.S., Zhang, P., Van Etten, R.A., and Tenen, D.G. (2000). Reversibility of acute B-cell leukaemia induced by BCR-ABL1. Nat. Genet. *24*, 57–60.

Jaiswal, S., Traver, D., Miyamoto, T., Akashi, K., Lagasse, E., and Weissman, I.L. (2003). Expression of BCR/ABL and BCL-2 in myeloid progenitors leads to myeloid leukemias. Proc. Natl. Acad. Sci. USA *100*, 10002–10007.

Jorgensen, H.G., Copland, M., Allan, E.K., Jiang, X., Eaves, A., Eaves, C., and Holyoake, T.L. (2006). Intermittent exposure of primitive quiescent chronic

myeloid leukemia cells to granulocyte-colony stimulating factor in vitro promotes their elimination by imatinib mesylate. Clin. Cancer Res. *12*, 626–633.

Kavalerchik, E., Goff, D., and Jamieson, C.H. (2008). Chronic myeloid leukemia stem cells. J. Clin. Oncol. *26*, 2911–2915.

Kogan, S.C., Ward, J.M., Anver, M.R., Berman, J.J., Brayton, C., Cardiff, R.D., Carter, J.S., de Coronado, S., Downing, J.R., Fredrickson, T.N., et al. (2002). Bethesda proposals for classification of nonlymphoid hematopoietic neoplasms in mice. Blood *100*, 238–245.

Kuhn, R., Schwenk, F., Aguet, M., and Rajewsky, K. (1995). Inducible gene targeting in mice. Science *269*, 1427–1429.

Lee, B.H., Tothova, Z., Levine, R.L., Anderson, K., Buza-Vidas, N., Cullen, D.E., McDowell, E.P., Adelsperger, J., Frohling, S., Huntly, B.J., et al. (2007). FLT3 mutations confer enhanced proliferation and survival properties to multipotent progenitors in a murine model of chronic myelomonocytic leukemia. Cancer Cell *12*, 367–380.

Li, L., Piloto, O., Nguyen, H.B., Greenberg, K., Takamiya, K., Racke, F., Huso, D., and Small, D. (2008). Knock-in of an internal tandem duplication mutation into murine FLT3 confers myeloproliferative disease in a mouse model. Blood *111*, 3849–3858.

Miyoshi, H., Shimizu, K., Kozu, T., Maseki, N., Kaneko, Y., and Ohki, M. (1991). t(8;21) breakpoints on chromosome 21 in acute myeloid leukemia are clustered within a limited region of a single gene, AML1. Proc. Natl. Acad. Sci. USA *88*, 10431–10434.

Neering, S.J., Bushnell, T., Sozer, S., Ashton, J., Rossi, R.M., Wang, P.Y., Bell, D.R., Heinrich, D., Bottaro, A., and Jordan, C.T. (2007). Leukemia stem cells in a genetically defined murine model of blast-crisis CML. Blood *110*, 2578–2585.

Oravecz-Wilson, K.I., Kiel, M.J., Li, L., Rao, D.S., Saint-Dic, D., Kumar, P.D., Provot, M.M., Hankenson, K.D., Reddy, V.N., Lieberman, A.P., et al. (2004). Huntingtin Interacting Protein 1 mutations lead to abnormal hematopoiesis, spinal defects and cataracts. Hum. Mol. Genet. *13*, 851–867.

Reilly, J.T. (2003). Receptor tyrosine kinases in normal and malignant haematopoiesis. Blood Rev. *17*, 241–248.

Ross, T.S., Bernard, O.A., Berger, R., and Gilliland, D.G. (1998). Fusion of Huntingtin interacting protein 1 to platelet-derived growth factor beta receptor (PDGFbetaR) in chronic myelomonocytic leukemia with t(5;7)(q33;q11.2). Blood *91*, 4419–4426.

Ross, T.S., and Gilliland, D.G. (1999). Transforming properties of the Huntingtin interacting protein 1/ platelet-derived growth factor beta receptor fusion protein. J. Biol. Chem. *274*, 22328–22336.

Savona, M., and Talpaz, M. (2008). Getting to the stem of chronic myeloid leukaemia. Nat. Rev. Cancer *8*, 341–350.

Sawyers, C.L., Gishizky, M.L., Quan, S., Golde, D.W., and Witte, O.N. (1992). Propagation of human blastic myeloid leukemias in the SCID mouse. Blood *79*, 2089–2098.

Schessl, C., Rawat, V.P., Cusan, M., Deshpande, A., Kohl, T.M., Rosten, P.M., Spiekermann, K., Humphries, R.K., Schnittger, S., Kern, W., et al. (2005). The AML1-ETO fusion gene and the FLT3 length mutation collaborate in inducing acute leukemia in mice. J. Clin. Invest. *115*, 2159–2168.

Sirard, C., Lapidot, T., Vormoor, J., Cashman, J.D., Doedens, M., Murdoch, B., Jamal, N., Messner, H., Addey, L., Minden, M., et al. (1996). Normal and leukemic SCID-repopulating cells (SRC) coexist in the bone marrow and peripheral blood from CML patients in chronic phase, whereas leukemic SRC are detected in blast crisis. Blood *87*, 1539–1548.

Tefferi, A., and Gilliland, D.G. (2007). Oncogenes in myeloproliferative disorders. Cell Cycle *6*, 550–566.

Wolff, N.C., and Ilaria, R.L., Jr. (2001). Establishment of a murine model for therapy-treated chronic myelogenous leukemia using the tyrosine kinase inhibitor STI571. Blood *98*, 2808–2816.

Yan, M., Kanbe, E., Peterson, L.F., Boyapati, A., Miao, Y., Wang, Y., Chen, I.M., Chen, Z., Rowley, J.D., Willman, C.L., and Zhang, D.E. (2006). A previously unidentified alternatively spliced isoform of t(8;21) transcript promotes leukemogenesis. Nat. Med. *12*, 945–949.

Yilmaz, O.H., Valdez, R., Theisen, B.K., Guo, W., Ferguson, D.O., Wu, H., and Morrison, S.J. (2006). Pten dependence distinguishes haematopoietic stem cells from leukaemia-initiating cells. Nature *441*, 475–482.